Large Eddy Simulation of the Sandia Flame E and F Using Dynamic Second-Order Moment Closure (DSMC) Model

Jianshan Yang, Kun Luo, Yun Bai, and JianRen Fan

Abstract

Turbulent piloted methane/air diffusion flames (Sandia Flame E and F) are evaluated using dynamic second-order moment closure (DSMC) model. The DSMC model is a combustion model for large eddy simulation, which is assumed that the model could be applied to both premixed flames and non-premixed flames. And the density fluctuation is taken into account. In the model, the averaged reaction rate is directly closed in the form of Arrhenius law. The third-order fluctuation correlations are neglected, and the second-order fluctuation correlations are closed using the algebraic form. All the coefficients in the model are evaluated dynamically. The results from simulation have been compared with the available measurement data. In general, there is good agreement between present simulations and measurements both for Sandia flame E and F, which gives a reasonable indication on the accuracy and adequacy of the DSMC model. And the further application is considerable for the model. The sub-grid effects in this combustion model have been studied. The reaction rate of methane for flame E is higher than the value of flame F and the sub-gird reaction rate is in the reverse value of its filtered reaction rate with 25 %. The sub-gird effects play an important role in this combustion model and should be treated carefully.

Keywords

Second-order • Turbulent combustion • Combustion model • Large eddy simulation

1 Introduction

There are increasing number of attentions that have been paid in large eddy simulation (LES) of combustion, which could give a more accurate result than Reynolds Averaged Navier Stokes (RANS) [1]. And the LES cost littler than the direct numerical simulation (DNS). It is complicated to simulation combustion using LES, due to that processes of reaction and molecular diffusion need to be concluded simultaneously. The combustion model and sub-grid scale stress model are needed in LES of combustion. A lot of combustion model have been proposed for LES to model combustion, in which, the most well-known combustion model are probability density function (PDF) model [2] and flamelet model [3]. The PDF combustion model is an accurate model and could be applied to the flame, which includes premixed and non-premixed flame. But the PDF model costs a lot of computational resource and need a mixing model, which is relatively simple and counts a lot in the PDF model. The flamelet model could predict non-premixed flame and premixed flame (with premixed flamelet approach) well, respectively. The most acceptable SGS stress models are Smagorinsky eddy-viscosity model [4], the dynamic kinetic energy model [5], and Germano dynamic model [6]. Recently, a dynamic second-order moment closure (DSMC) model, which could deal with the premixed flame and non-premixed flame, is proposed by the present authors. This paper is aimed to demonstrate the ability of the DSMC model. The Sandia flame E and F have

J. Yang (✉) · K. Luo · Y. Bai · J. Fan
State Key Laboratory of Clean Energy Utilization, Zhejiang University, Hangzhou 310027, Zhejiang, People's Republic of China
e-mail: yangjianshan@zju.edu.cn

G. Yue and S. Li (eds.), *Clean Coal Technology and Sustainable Development*,
DOI 10.1007/978-981-10-2023-0_15

been selected to check the model. The time-averaged and its rms value of the statistic data are studied and the sub-grid effects in DSMC model also will be conducted.

2 Mathematical Model

In this paper, the filtered conservation equations are as follows:

Momentum equation

$$\frac{\partial \bar{\rho}}{\partial t} + \frac{\partial(\bar{\rho}\tilde{u}_i)}{\partial x_i} = 0 \tag{1}$$

Momentum equation

$$\frac{\partial(\bar{\rho}\tilde{u}_i)}{\partial t} + \frac{\partial\left(\bar{\rho}\tilde{u}_i\tilde{u}_j\right)}{\partial x_j} = -\frac{\partial \bar{p}}{\partial x_i} + \frac{\partial \bar{\sigma}_{ij}}{\partial x_j} - \frac{\partial}{\partial x_j}\left[\bar{\rho}(\widetilde{u_i u_j} - \tilde{u}_i\tilde{u}_j)\right] \tag{2}$$

And scalar equation

$$\frac{\partial\left(\bar{\rho}\tilde{\phi}_k\right)}{\partial t} + \frac{\partial\left(\bar{\rho}\tilde{\phi}_k\tilde{u}_j\right)}{\partial x_j} = \frac{\partial}{\partial x_j}\left(\bar{\rho}\tilde{D}_k\frac{\partial\tilde{\phi}_k}{\partial x_j}\right) + \frac{\partial}{\partial x_j}\left[\bar{\rho}(-\widetilde{\phi_k u_j} + \tilde{u}_j\tilde{\phi}_k)\right] + \overline{\omega_k} \tag{3}$$

In this simulation ϕ_k are species and Sutherland's three coefficient law is applied to compute the molecular viscosity. The Lewis number is equal to unity. So, the $\bar{\rho}\tilde{D}_k$ are the same for all of the scalar and could be equal to

$$\lambda/C_p = 2.58 \times 10^{-5}(\mathrm{T}/298\,\mathrm{K})^{0.69}\ \mathrm{kg\,m^{-1}\,s^{-1}} \tag{4}$$

where λ is the thermal conductivity and C_p is the specific heat [7].

The SGS stress is calculated with an eddy viscosity assumption,

$$\bar{\rho}(-\widetilde{u_i u_j} + \tilde{u}_i\tilde{u}_j) = 2\mu_t\tilde{S}_{ij} - \frac{1}{3}\bar{\rho}q^2\delta_{ij} \tag{5}$$

where $\bar{\rho}q^2 = C_k\bar{\rho}\Delta^2\left|\tilde{S}\right|^2$ and

$$\tilde{S}_{ij} = \frac{1}{2}\left(\frac{\partial\tilde{u}_i}{\partial x_j} + \frac{\partial\tilde{u}_j}{\partial x_i}\right) - \frac{1}{3}\delta_{ij}\frac{\partial\tilde{u}_k}{\partial x_k} \tag{6}$$

The eddy viscosity is computed with the Smagorinsky model [8].

In this paper, the filtered reaction rate $\overline{\omega_k}$ is computed by Arrhenius law with the DSCM model. The global reaction chemical mechanism is followed.

$$\overline{\dot{w}_1} = \overline{A\exp(-E/RT)\left(\rho\frac{Y_F}{W_F}\right)^m\left(\rho\frac{Y_O}{W_O}\right)^n} = \overline{KR_1^m R_2^n} = (\overline{KR_1}^m\overline{R_2}^n + \overline{\dot{w}_{sgs}}) \tag{7}$$

$$\overline{\dot{w}_{sgs}} = mn\overline{R_1}^{m-1}\overline{R_2}^{n-1}\overline{KR_1'R_2'} + m\overline{R_1}^{m-1}\overline{R_2}^{n}\overline{K'R_1'} + n\overline{R_1}^{m}\overline{R_2}^{n-1}\overline{K'R_2'} \tag{8}$$

where $K = A\left(\frac{1}{W_F}\right)^m\left(\frac{1}{W_O}\right)^n\exp(-\frac{E}{RT})$, $R_1 = \rho Y_F$, $R_2 = \rho Y_O$ the subscripts F is fuel and subscripts F is oxidant. The m and n are the exponents of concentration, which mainly depends on the chemical kinetics. W and Y stand for the molecular weight and mass fraction, respectively. E stands for activation energy. R and A stand for universal gas constant and exponential factor. The $\overline{K}$ is a highly nonlinearity exponential function and could be model through a top-hat PDF as follows:

$$\bar{K} = \frac{1}{2}\left\{\exp\left[-\frac{E}{R\left(\bar{T} + \overline{T'^2}^{1/2}\right)}\right] + \exp\left[-\frac{E}{R\left(\bar{T} - \overline{T'^2}^{1/2}\right)}\right]\right\} \tag{9}$$

The sub-grid variance model [8] is applied to model the variance of temperature in Eq. 9. The algebraic expression is used to compute the sub-grid term in Eq. 8.

$$\overline{\phi'\varphi'} = C_{\phi\varphi}\frac{\partial\overline{\phi}}{\partial x_j}\frac{\partial\overline{\varphi}}{\partial x_j} \tag{10}$$

where the φ and ϕ stand for R_1, R_2, or K. All of the coefficients in this paper are computed through the dynamic procedure [8].

3 Calculations Details

Sandia Flame series E and F [9], piloted methane/air non-premixed turbulent jet flame, are conducted in this paper. At first, the burner would be introduced; the diameter of the central jet is of 7.2 mm and the outer diameter is of 18.2 mm. The jet fuel is 75 % air and 25 % CH_4 in volume and the stoichiometric mixture fraction is of Zst = 0.351. The bulk jet velocities are 74.4 and 99.2 m/s for the flame E and flame F, respectively. And the corresponding velocity of

the pilot flame, a mixture of C_2H_2, H_2, air, CO_2, and N_2 with an equivalence ratio of 0.77, are 11.4 and 22.8 m/s. The velocity of co-flow air is 0.9 m/s. In this simulation, the temperature of piloted flame are 1880 K for flame E and 1830 K for flame F. Cylindrical simulation domain with an axial length of 0.6 m (about 83D) and a radius of 0.072 m (10D) is selected. The mesh used here is consisted of 300 × 120 × 64 in axial, radial, and azimuthal direction. The mesh is stretched in axial and radial direction. A one-step irreversible reaction is applied here as chemical kinetics mechanism [10].

4 Result and Discussion

In the rest part of this paper, the time average result from this large eddy simulation would be conducted and compared with experimental data. The statistic data is obtained through sampling over ten flow-through period, where the flow-through period is defined as the time flow flowing through all the computational zone along the centerline in the jet bulk velocity. To begin with, the mean and rms data of velocity, temperature, and mixture fraction are selected to compare the measurement data. The data from typical zone with strong extinction, X = 7.5D; re-ignition, X = 15D, and re-ignition completed zone, X = 30D, have been selected to verify the models.

The radial profile of the mean and rms value for flame E and F are given in Fig. 1. It is noted that both mean and rms velocity are in reasonable agreement with the measurement data for the flame E and F, although the mean velocity is somewhat underestimated at X = 7.5D for flame F, which may be caused by the inflow boundary conditions. Figure 2 gives the radical profile of mean and rms temperature at three axial locations for flame E and F. In general, the results of temperature from this simulation are reasonably in good agreement with the experimental data, although the maximum mean temperature from both flame E and flame F have been over predicted by around 400 K, which is associated with two reasons. One is the one-step irreversible chemical mechanism is applied in the present study. The other is the extinction is not captured due to the absence of the intermediate species.

Figure 3 shows radial profiles of mean and rms mixture fraction at three axial locations for flame E and F. The values of mean mixture fraction and rms mixture fraction agree

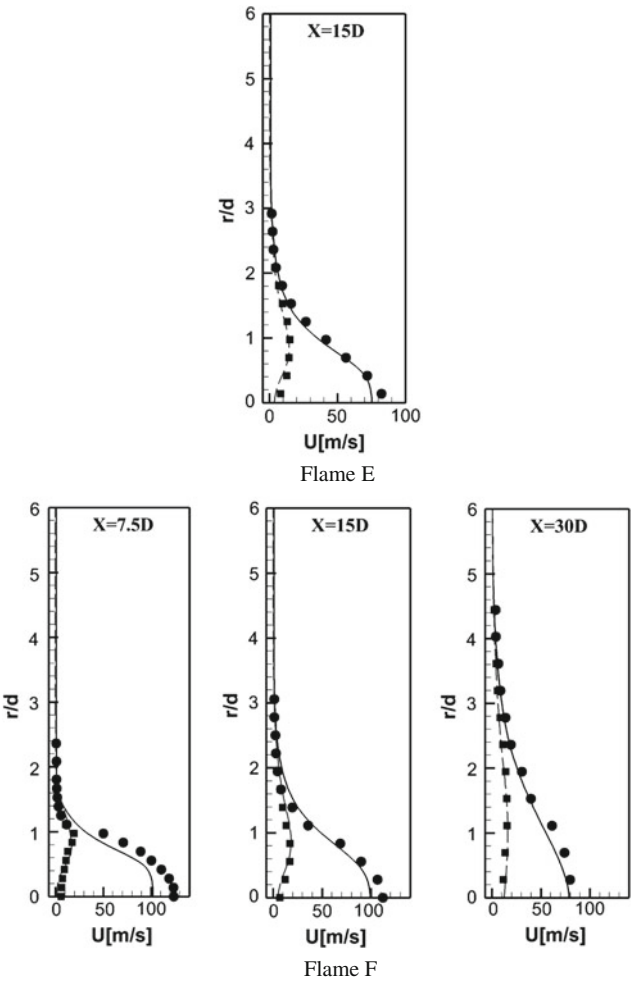

Fig. 1 Radial profiles of mean and rms velocity at three axial locations for flame E and F. The symbols of *circle* and *square* denote mean and rms data of experiment. The *solid lines* denote the mean value of simulation. And the *long dash line* denotes the rms value of simulation

with the measurement very well for flame E, and for Flame F, the value of mean mixture fraction somewhat have been overpredicted in X = 30D.

At the next part, the sub-grid effects in this combustion model will be conducted carefully. The filter reaction rate and its sub-grid reaction rate for methane are selected to study with the data at six axial position (X = 2D, X = 3D, X = 7.5D, X = 15D, X = 30D, and X = 4.5D).

The radial profiles of filter reaction rate and its sub-gird reaction rate are depicted in Fig. 4. It is interesting to find that the filter reaction rate of methane for flame E is slightly higher than the value for flame F except the value in the

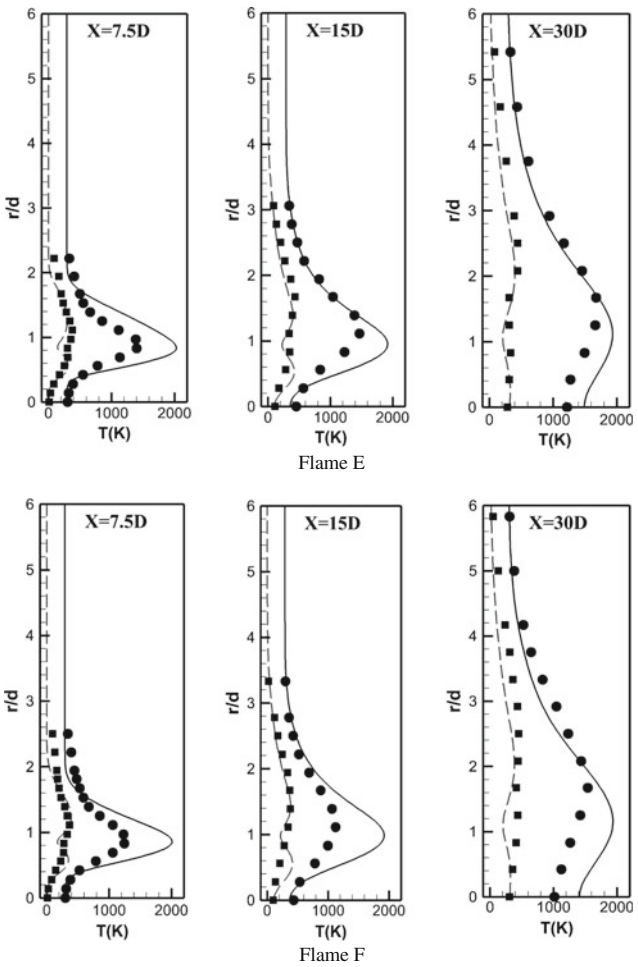

Fig. 2 Radial profiles of mean and rms temperature at three axial locations for flame E and F. The symbols of *circle* and *square* denote mean and rms data of experiment. The *solid lines* denote the mean value of simulation. And the *long dash line* denotes the rms value of simulation

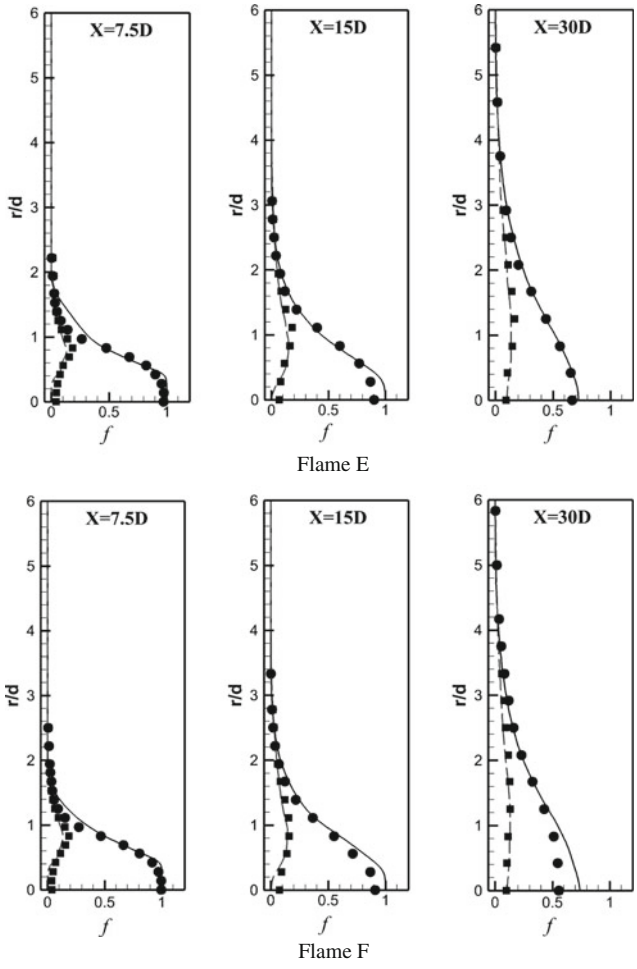

Fig. 3 Radial profiles of mean and rms mixture fraction at three axial locations for flame E and F. The symbols of *circle* and *square* denote mean and rms data of experiment. The *solid lines* denote the mean value of simulation. And the *long dash line* denotes the rms value of simulation

position of $X = 45D$. This indicates that consumption of methane for flame E is faster than the flame F do. And the flame length of flame E is shorter than the flame length of flame F. This may be due to the reason that the jet velocity of flame F is faster than the jet velocity of flame E, which would has the results that the heat diffusion process and molecular mixing of flame F is more quickly than Flame E do. At the position of $X = 45D$, the reaction rate of flame E equals to zero while flame F has slow reaction. It is noted that the sub-grid reaction rate make inverse contribution to its filtered reaction rate with the value of around 25 % for both flame E and flame F and the peak value of sub-grid reaction rate and its filtered reaction rate are in the same position.

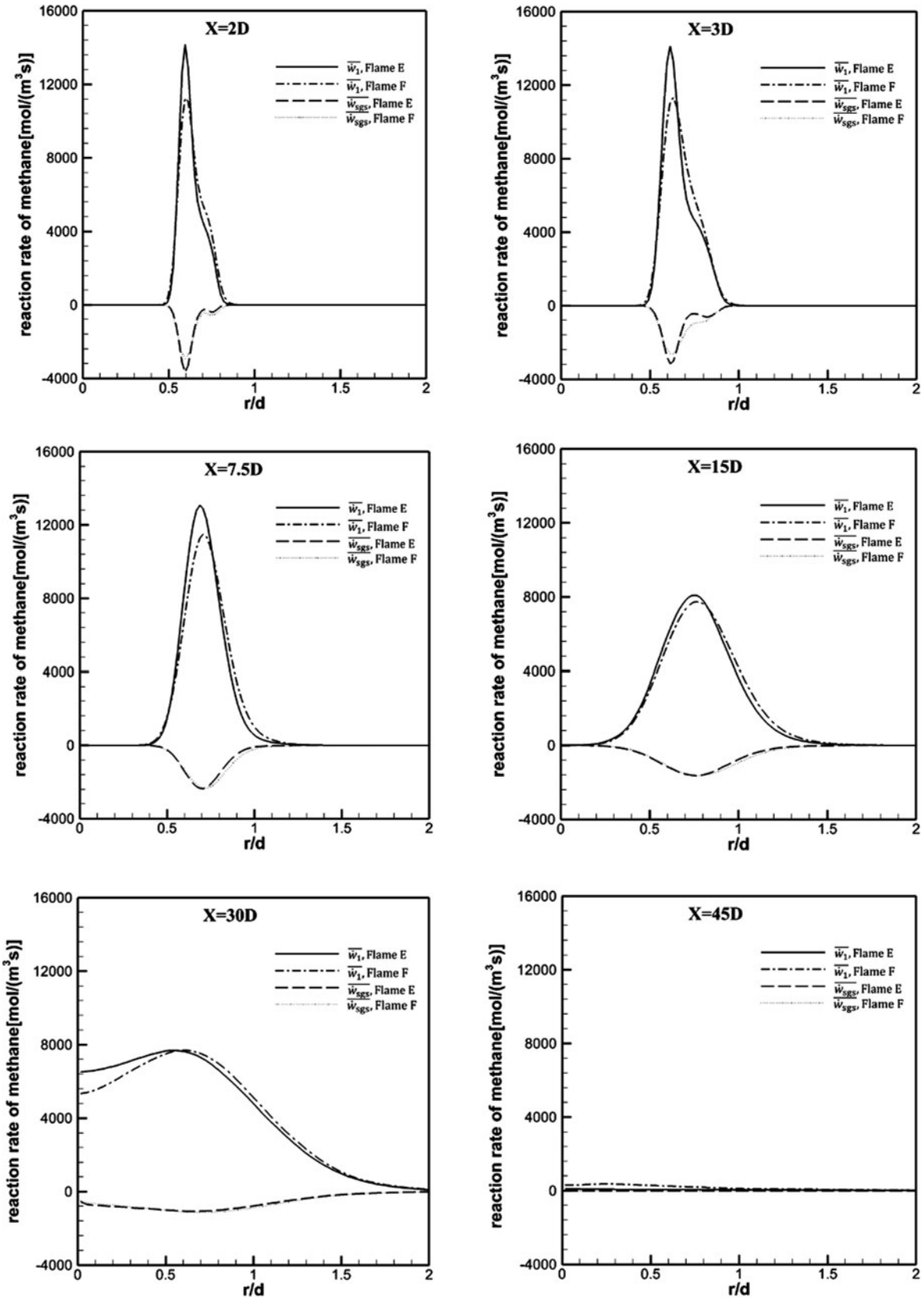

Fig. 4 Radial profiles of filtered reaction rate and its sub-grid reaction rate of methane at three six locations(X = 2D, X = 3D, X = 7.5D, X = 15D, X = 30D, and X = 4.5D) for flame E and F. The *solid line* and *dash dot line* denote the filtered reaction rate of methane for flame E and F, respectively. The *long dash line* and *dotted line* represent the sub-gird reaction rate of methane for flame E and flame F

5 Conclusion

Turbulent piloted methane/air diffusion flames (Sandia Flame E and F) are studied using Dynamic Second-order Moment Closure (DSMC) model. The DSMC model is a combustion model for large eddy simulation, which is assumed that the model could be applied to both premixed flames and non-premixed flames. The results from simulation have been compared with the available measurement data. In general, there is good agreement between present simulations and measurements both for Sandia flame E and F, which gives a reasonable indication on the accuracy and adequacy of the DSMC model. The sub-grid effects in this combustion model have been studied. The reaction rate of methane for flame E is higher than the value of flame F. and the sub-gird reaction rate is in the reverse value of its filtered reaction rate with 25 %. The sub-gird effects play an important role in this combustion model and should be treated carefully.

Acknowledgments This work was supported by the National Natural Science Foundation of China (Grant Nos. 51222602, 51176170, 51390490). The authors gratefully thanks to the kindness discussion with Professor Lixing Zhou.

References

1. Pitsch H (2006) Large-eddy simulation of turbulent combustion. Ann Rev Fluid Mech 38:453–482
2. Pope SB (1985) PDF methods for turbulent reactive flows. Prog Energy Combust Sci 11(2):119–192
3. Peters N (1984) Laminar diffusion flamelet models in non-premixed turbulent combustion. Prog Energy Combust Sci 319–339
4. Smagorinsky J (1963) General circulation experiments with the primitive equations: I. The basic experiment. Mon Weather Rev 91:99–164
5. Kim WW, Menon S, Mongia HC (1999) Large-eddy simulation of a gas turbine combustor flow. Combust Sci Technol 143:25–62
6. Germano M, Piomelli U, Moin P, Cabot WH (1991) A dynamic sub-grid-scale eddy viscosity model. Phys Fluids A 3:1760
7. Smooke MD, Giovangigli V (1991) In: Smooke MD (ed) Reduced kinetic mechanisms and asymptotic approximations for methane-air flames. Springer, Berlin, pp 1–28
8. Pierce CD, Moin P (2004) Progress-variable approach for large-eddy simulation of non-premixed turbulent combustion. J Fluid Mech 504:73–97
9. Barlow RS, Frank JH (1998) Effects of turbulence on species mass fractions in methane/air jet flames. Symp (Int) Combust 27(1): 1087–1095
10. Westbrook CK, Dryer FL (1981) Simplified reaction mechanisms for the oxidation of hydrocarbon fuels in flames. Combust Sci Technol 27:31–43